

A NOVEL MODEL OF PZT ACTUATOR AND ITS APPLICATION IN HYSTERESIS AND VIBRATION CONTROLS

Bashir Bala Muhammad^a, Md Habibur Rahman^a, Mohd Ridzuan Ahmad^{a*}, Muhammad Bashir^b

^aDepartment of Control and Mechatronics Engineering, Faculty of Electrical Engineering, Universiti Teknologi Malaysia, 81310 UTM Johor Bahru, Malaysia

^bSchool of Electro-Mechanical Engineering, Xidian University, Xi'an, China

Article history

Received

2 July 2015

Received in revised form

5 November 2015

Accepted

17 March 2016

*Corresponding author

ridzuan@fke.utm.my

Abstract

The piezoelectric actuator is a voltage spring system that behaves in a similar characteristic to mechanical mass spring system. The displacements profile of the piezoelectric actuator shifts due to hysteresis and creep during actuation. The static (non-dynamics) models of piezoelectric actuator developed in the past consisted of a number of equations which could not be simplified in the form of a single transfer function. Furthermore, the modelling of dynamic (vibrating) piezoelectric actuator was not considered. In this work, we present the behaviour of the piezoelectric actuator in terms of mechanical displacement from applied electric potential. The single transfer function mathematical model is generated representing the actuator characteristics. The dynamic (vibration) model that can vibrate at a desired frequency of the actuator is also developed. The models are developed by system identification from experimental results. A high resolution microscope together with the image processing technique were used to obtain the system characteristics. Simulation using Matlab Simulink is used to validate the experiment (The hysteresis was reduced by 90 % and the vibration was reduced to 97 %).

Keywords: Dynamic piezoelectric actuator; PID controller; piezoelectric actuator; non-dynamic piezoelectric actuator; voltage spring system

© 2016 Penerbit UTM Press. All rights reserved

1.0 INTRODUCTION

Piezoelectric actuator (PZT) is a displacement transducer that converts electrical signals to physical displacement. As a capacitive actuator, it consumes less energy in generating a force while maintaining a steady position. In contrast, the electromagnetic actuator consumes energy and generates heat, therefore it is often accompanied by heat sink. The capacitive nature of the PZT is used to increase serial stiffness, reduce parallel stiffness, eliminate friction from the contact surface, and increase the work round by preloading piezoelectric stack actuator [1]. These are its advantages over mechanical actuators where it reduces energy intake and decreases heat generation of the system. Boring bar vibration was curbed by hybrid absorber, piezoelectric actuator and LR circuit [2], which was validated using a cutting

test. The CNC cutting lathe machine vibration was controlled by means of out-of-phase control signals during turning with the use of dSpace [3]. Even though there were limitations arising due to the rigidity of the cutting tools, the roughness was significantly improved by the use of the piezoelectric actuator.

The self-excited undesired vibration associated with the turning process is called chatter. It results in production problems such as poor surface finish and reduce work quality in machining. Adaptive control law was employed to effectively control the vibration of the turning process by using piezoelectric actuator [4]. The displacement between the cutting tool and work piece was minimized during the turning process. The minimum variance was used for self-turning control to suppress the vibration of the cantilever beam [5]. The control voltage was applied to the PZT

when the beam was subjected to vibration from the environment.

The vibration of flexible linkage mechanism using PZT was discussed [6]. The vibration of flexible structure was controlled using fuzzy logic controller and piezoelectric actuator. About 33 % of the vibration was restricted.

Hysteresis properties in PZT was modelled based on back propagation neural network, Nonlinear Autoregressive Moving average with exogenous input (NARMAX) [7]. The controller can track unstable random motion. It is also suitable for precision motion control. The finite element method and Hamilton's principle outline the linear response of piezo-thermo-elastic plate [8]. It stated that an increase in temperature causes a corresponding increase in the vibration amplitude. The control voltage was used to minimise the structural vibration in a laminated thermoelectric plate. The Bouc-Wen hysteresis model was used to describe the piezoelectric properties in [9]. The system identification (system ID) procedure was used to generate dynamic and non-dynamic model of PZT in [10], and controlled by PID controller.

The servo system was coupled with piezoelectric actuator in electrical discharge machining/grinding (EDM/EDG) to achieve precision machining in [11].

The piezoelectric actuator micro positioning was discussed in [12]–[21]. Piezoelectric based micro positioning was established by sandwich model [12], PZT film [13], BAT search algorithm [14], Cr-N thin film displacement sensor [15], micro-displacement amplifier (RMDA) [16], Prandtl-Ishlinskii model [17], grinding table with piezoelectric voltage feedback [18], neural net-based cross coupling based on Preisach model [19], spring-mounted PZT [20], and hard disk head positioning system [21].

The piezoelectric actuator was employed as micro actuator in [22]–[24], for position magnetic head element [22], to generate linear and curvilinear motion [23], and based on Donnell–Mushtari–Vlasov theory on rocket conical shell actuation [24].

Piezoelectric actuator was also engaged in microfluidic [25]–[31], for example as valve-less piezoelectric micro pump [25], [28], [30], peristaltic micro pump in thin film PZT with active micro valves [29], PZT peristaltic micro pump [27], droplet based micro fluidic device [26], and serial connection multi-chamber PZT pump [31].

The modelling of PZT in this work will be based on system identification techniques. This paper will model both dynamic (vibrating) and non-dynamic (static) piezoelectric actuator. It will consider the control of actuator using PID controller.

2.0 EXPERIMENTAL METHOD

2.1 Determine The Hysteresis Model Of Piezoelectric Actuator (Non-Dynamic Model)

The experiment was conducted to determine the characteristics of the piezoelectric actuator based on system characteristics using Resin-coated type AE series actuator. A high resolution microscope was used to detect the displacement when staircase DC voltage was applied to the piezoelectric actuator. Images captured by a camera were processed to obtain the displacement for various input DC voltage. The images were processed to determine the displacements using image processing techniques. The input and output characteristics were obtained and tabulated in Table 1. The system model was generated using system identification techniques of Matlab. Figure 1 shows the experiment setup, where the actuator was mounted on the microscope camera to capture the images. Fig. 2 shows image acquisition and model development from a computer system. The images were processed and used in Matlab system identification tool box. Table 1 shows the displacement obtained at different voltage of non-dynamic model of PZT. The table consists of two parts. Part 1 provides the relationship that existed between DC voltage and displacement; the DC voltage increment from 0 V to 125 V and the corresponding displacements in micrometre were recorded. While part 2 provides the relationship between decreasing DC voltage from 125 V to 0 V and the corresponding displacements in micrometre were also recorded. Fig. 3 shows the relationship between the system input and output data with time during loading and unloading phases of non-dynamic PZT model. In the loading phase the DC voltage was applied to the actuator in the stair case incremental step; the actuator extended in length when the voltage increased until it reached its full length at maximum voltage. In the unloading phase the actuator was fully extended at maximum voltage. The maximum voltage would be reduced gradually and periodically until the actuator returned to the rest state at minimum volt. Fig. 4 shows the hysteresis and nonlinear hysteresis characteristics while Fig. 5 shows the step response that compares between the actual and estimated non-dynamic PZT model.



Figure 1 Section 1 is DC voltage generator. Section 2 is inverted microscope. Section 3 presents PZT actuator focused by camera. Section 4 is image and video processing using computer. The actuator is supplied with DC voltage directly from DC power supply and the corresponding images are captured at different voltage. The images and videos are stored in a computer system.

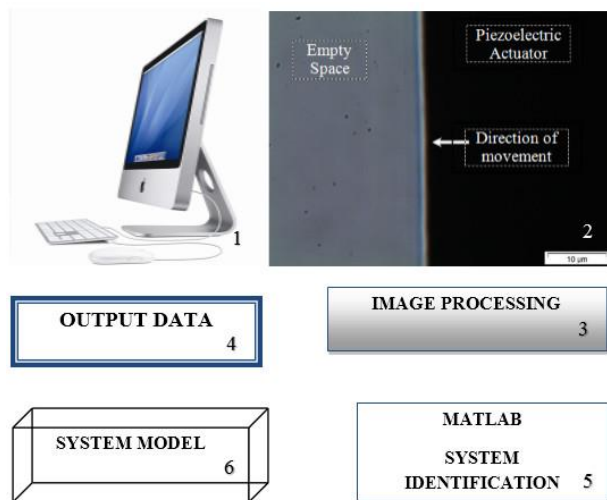


Figure 2 Section 1 is the computer for image and video recording. Section 2 is the sample image obtained. Section 3 is the image processing by computer software. Section 4 is the output data to be used in Matlab. Section 5 is the Matlab system identification tool box for model development. Section 6 is the developed mathematical model. The image was captured and processed by image processing software to obtain the output data. The input and output data were used to develop the model using system identification techniques of Matlab.

2.2 Table Of Results

The table below displays the result of hysteresis during loading and unloading phase of non-dynamic model. Part 1 shows the actuator voltage and corresponding displacement during loading phase while part 2 displays the actuator voltage and corresponding displacement during unloading phase.

Table 1 Results

PZT S/no	PART 1		PART 2	
	Voltage (V)	Displacement (µm)	Voltage (V)	Displacement (µm)
1	0	0	125	2.671
2	5	0.079	120	2.599
3	10	0.152	115	2.519
4	15	0.305	110	2.442
5	20	0.381	105	2.366
6	25	0.458	100	2.213
7	30	0.61	95	2.137
8	35	0.687	90	2.137
9	40	0.839	85	1.984
10	45	0.992	80	1.904
11	50	1.068	75	1.832
12	55	1.221	70	1.755
13	60	1.297	65	1.603
14	65	1.45	60	1.526
15	70	1.526	55	1.45
16	75	1.679	50	1.297
17	80	1.829	45	1.221
18	85	1.908	40	1.068
19	90	1.984	35	0.919
20	95	2.061	30	0.763
21	100	2.137	25	0.687
22	105	2.29	20	0.61
23	110	2.366	15	0.458
24	115	2.439	10	0.305
25	120	2.595	5	0.076
26	125	2.671	0	0

2.3 Mathematical Modelling (Non-Dynamic Model)

Equation (1) shows the mathematical model of the system from non-dynamic model. The system poles are at $-0.4185 \pm 2.2833i$ & $-0.6817 \pm 0.9063i$.

$$G(s) = \frac{0.07962s + 0.1521}{s^4 + 2.201s^3 + 7.816s^2 + 8.423s + 6.93} \tag{1}$$

The transfer function of the system is the linear system model and shows that the system fits the estimation data with 91.5% with final prediction error (FPE): 0.00586989.

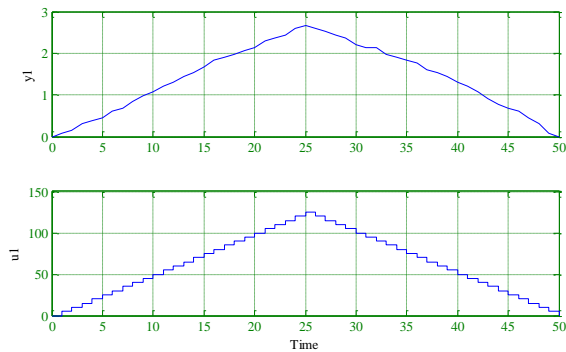


Figure 3 The output (y1) and input (u1) verses time of the system

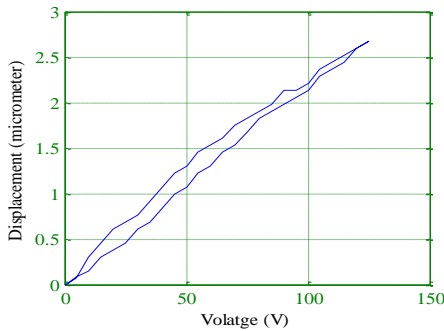


Figure 4 Hysteresis of piezoelectric actuator. The nonlinear hysteresis characteristics of the actuator can be observed from the graph

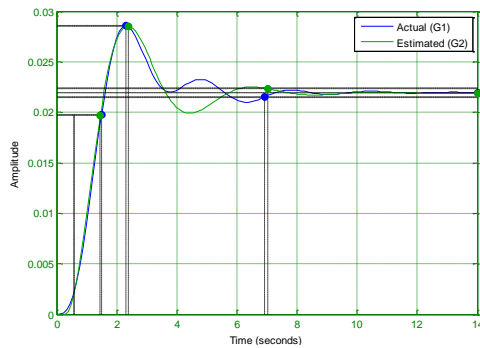


Figure 5 Step Response of actual and estimated Model of non-dynamic PZT model. It can be seen that both model have similar characteristics

2.4 Experiment for Vibration (Dynamic Model)

The dynamic PZT is vibrating at certain frequency based on the program written on Arduino microcontroller. The output of the Arduino microcontroller is also amplified by the amplifier before supplying it to the actuator. The displacement of the actuator is proportional to the actuator input voltage. The videos were captured and processed from the vibrating actuator to obtain the output data. The input and output data were used in Matlab system identification tool box to generate the dynamic model. Figure 6 contains the setup for generating the vibration of dynamic PZT. Figure 7 represents the setup for image and video processing of dynamic PZT model.

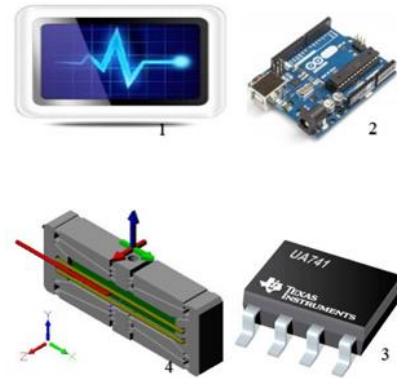


Figure 6 Setup for generating Vibration, Section 1 shows the computer system which contains Arduino software, section 2 display the Arduino microcontroller. Section 3 contains UA741 amplifier. Section 4 contains piezoelectric actuator. The C program was sent from the computer to the Arduino microcontroller that generates output voltage for 5000ms and delays of 5000ms and transfers it to the UA741 amplify input based on resistance gain. The amplifier generates square wave voltage from 18 V to 50 V which generates the vibration in the PZT actuator.



Figure 7 Setup for image and video processing. Section 1 displays the computer system which captures images and videos from the actuator. Section 2 shows image and video processing using image and video processing software. Section 3 shows system identification from Matlab interface. Section 4 is the system model developed from Matlab system identification tool box.

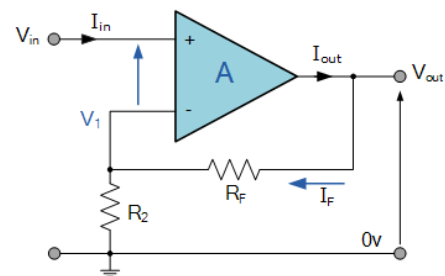


Figure 8 UA741 Amplifier Circuit. The resistance R_1 and R_2 were used for voltage amplification.

2.4.1 Operational Amplifier

The circuit in Figure 8 shows non-inverting amplifier used to amplify the voltage to the desired output in the experiment. R_f/R_2 is the gain of the amplifier. The

gain is used to amplify the input voltage to the required output. Equation (2) shows the relationship between the gain, input and output voltage. While Equation (3) show the relationship between voltage, slew rate and frequency. Figure 8 displays the amplifier circuit. The circuit was used to amplify the Arduino output voltage from 5 V to 50 V. Table 2 displays the data output of image and video processing from dynamic PZT model. Figure 9 displays the time response obtained from Matlab using the data from Table 2. The input of the system is square wave as shown in Figure 9. The square wave was generated by using Arduino microcontroller and amplifier. Figure 10 shows the comparison between the actual and estimated systems. To amplify 5 volts to 50 volts we need to calculate the gain.

$$V_{out} = V_{in} \left(\frac{R_f}{R_2} + 1 \right) \tag{2}$$

$$V_{out} = 50v ; V_{in} = 5v ,$$

$$Gain = \frac{R_f}{R_2} = \frac{50}{5} - 1 = 10 - 1 = 9$$

$$slewrate = 2\pi f v \tag{3}$$

$$Frequency = \frac{slew\ rate}{2\pi v}$$

$$UA741\ Slew\ rate = 0.5, V = 5v, \\ F = (0.5 * 1000) / (2\pi v) = 15.91\ KHz$$

2.4.2 Vibration Model Results

Table 2 displays the result of vibrating piezoelectric actuator at 1.01626 Hz. The input voltage and corresponding output displacement were shown.

Table 2 Vibration model results

S/No	Freq.(Hz)	Output (µm)	Input (V)
1	1.01626	11.224	18
2	1.01626	11.224	18
3	1.01626	12.245	50
4	1.01626	12.245	50
5	1.01626	11.224	18
6	1.01626	11.224	18
7	1.01626	12.245	50
8	1.01626	12.245	50
9	1.01626	11.224	18
10	1.01626	11.224	18

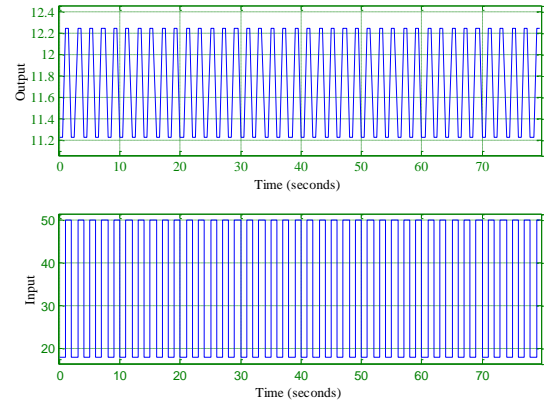


Figure 9 The system input and output verses time was obtained when the data from Table 2 was processed in the Matlab system identification tool box. The input is square wave form with its amplitude determined by the magnitude of the applied voltage. The output is a vibration as depicted by output verses time.

2.5 Mathematical Model for Vibration

Vibration Transfer Function of Actual Model

Equation (4) represents the mathematical model of the actual dynamic PZT. This equation was developed from the experimental data (Table 2) using the system ID tool of Matlab. Equation (4) was simplified using general second order model of Equation (5) to obtain its simplified version in Equation (6).

$$G(s) = \frac{-0.02777s - 0.06457}{s^2 + 0.1157s + 0.2176} \tag{4}$$

Estimated Transfer Function Model

Equation (5) represents the general second order equation. Equation (6) is the transfer function representing the estimated model derived from Equation (4).

$$G(s) = \frac{k}{s^2 + 2\xi w_n s + w_n^2} \tag{5}$$

$$G(s) = \frac{-0.0722}{s^2 + 0.1187s + 0.243} \tag{6}$$

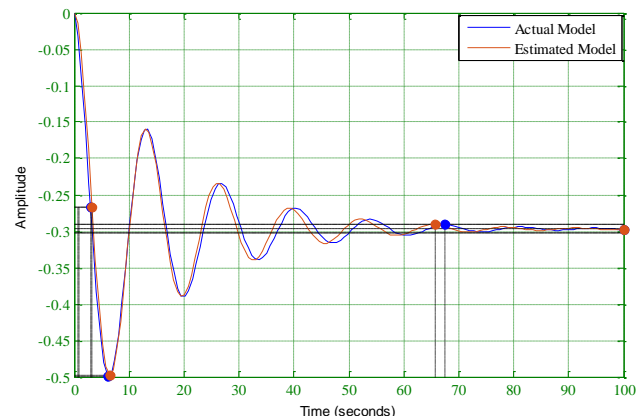


Figure 10 Comparison between actual and estimated models of dynamic PZT. The response indicates that the estimated model has similar characteristics as the actual model.

2.6 Controllability and Observability

2.6.1 Hysteresis Model

The estimated hysteresis model in state space form is represented in Equations (7) and (8).

$$\dot{X}_1 = \begin{bmatrix} -1.1577 & -2.6439 \\ 1 & 0 \end{bmatrix} x(t) + \begin{bmatrix} 1 \\ 0 \end{bmatrix} u(t) \quad (7)$$

$$Y_1 = [0 \quad 0.0579] x(t) \quad (8)$$

Equation (9) is the controllability matrix formula. Equation (10) is the controllability matrix of the hysteresis model. The system is controllable as the matrix is non-singular with full row rank of 2.

$$G^c = [B \quad AB] \quad (9)$$

$$G^{c1} = \begin{bmatrix} 1 & -1.1577 \\ 0 & 1 \end{bmatrix} \quad (10)$$

The observability matrix formula is represented in Equation (11). Equation (12) represents the observability matrix of the system. The equation shows that the system is observable because it is non-singular with full column rank of 2.

$$G^o = \begin{bmatrix} C \\ CA \end{bmatrix} \quad (11)$$

$$G^{o1} = \begin{bmatrix} 0 & 0.0579 \\ 0.0579 & 0 \end{bmatrix} \quad (12)$$

2.6.2 Vibration Model

The vibration model of the system in state space is represented in Equations (13) and (14).

$$\dot{X}_2 = \begin{bmatrix} -0.1187 & -2.430 \\ 1 & 0 \end{bmatrix} x(t) + \begin{bmatrix} 1 \\ 0 \end{bmatrix} u(t) \quad (13)$$

$$Y_2 = [0 \quad -0.0722] x(t) \quad (14)$$

The controllability of the system is computed and the system is controllable because it is non-singular matrix with full row rank of 2 as represented in Equation (15).

$$G^{c2} = \begin{bmatrix} 1 & -0.1187 \\ 0 & 1 \end{bmatrix} \quad (15)$$

The observability of the system is determined using observability matrix as shown in Equation (16). The system is observable because it is non-singular matrix with full column rank of 2.

$$G^{o2} = \begin{bmatrix} 0 & -0.0722 \\ -0.0722 & 0 \end{bmatrix} \quad (16)$$

The systems are found to be controllable and observable. Therefore, we proceed to the controller design in the next section.

2.7 Controller Design

The proportional integral and derivative (PID) controller consists of the combination of proportional (K_p), integral (K_i), and derivative (K_d) control action. The proportional controller is amplifier with an adjustable gain. It reduces the rise time but does not

eliminate steady state error. While an integral controller eliminates steady state error for constant or step input but may make the transient response slower. Whereas the derivative controller will increase the stability of the system, reduce the overshoot and improve the transient response. Equation (17) represents the mathematical description of a PID controller. The PID controller for hysteresis was designed based on Equation (1) non-dynamic model of the PZT using Matlab Simulink interface. The PID controller for vibration was designed based on Equation (4) dynamic model of the PZT using Matlab Simulink interface. The estimated simplified second order equation can also be used for both Equations (1) and (4) for controller design in Matlab Simulink interface. Therefore, Equation (6) can be used instead of Equation (4) as the two equations have similar characteristics as shown in Fig. 10. Figure 11 represents a block diagram of the PID controller.

$$u(t) = K_p e(t) + \frac{K_p}{T_i} \int_0^t e(t) dt + K_p T_d \frac{de(t)}{dt} \quad (17)$$

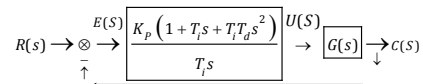


Figure 11 Block diagram of PID controller. $R(s)$ is the input voltage (reference input). $E(s)$ is the error signal. $U(s)$ is the output of the controller. $U(s)$ becomes input to the PZT. $G(s)$ is the system (PZT actuator). $C(s)$ is the system output (displacement). K_p is the proportional gain, T_i is the integral time, and T_d is the derivative time.

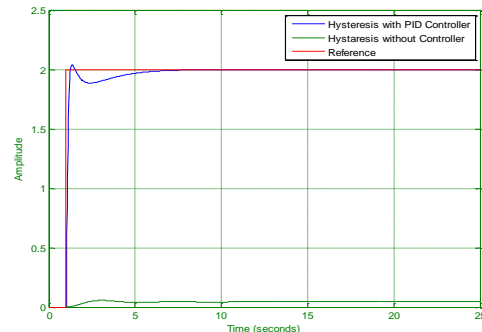


Figure 12 The step responses of hysteresis (non-dynamic) model controlled with PID controller and without controller

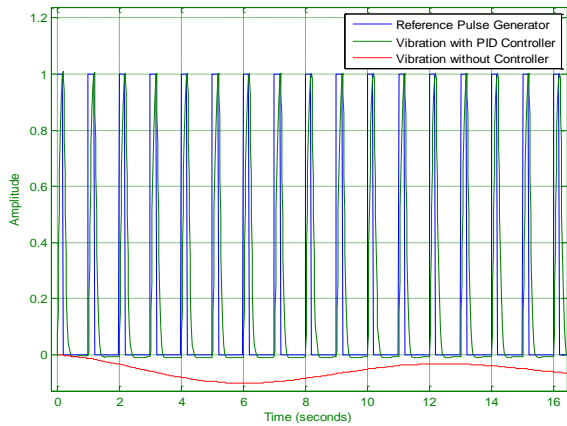


Figure 13 Comparison between vibration (dynamic) model with PID controller and the one without controller using pulse generator input. The graph shows the PID controller generates the control output with the desired amplitude to produce the desired micro actuation.

2.7.1 PID Controller for Hysteresis

A PID controller was used in this experiment to control hysteresis of PZT (non-dynamic model) Equation (1). Figure 12 compare the step response of the actuator with and without PID controller. Whereas with controller tracked the reference input while without controller did not.

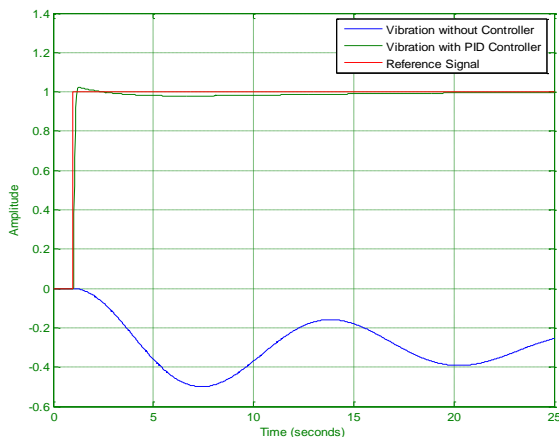


Figure 14 Comparison between vibration (dynamic) model with PID controller and the one without controller using step input. The PID controller provides the desired displacement of the actuator as can be seen from the graph.

2.7.2 PID Controller for Vibration Control

The PID parameters were tuned using Matlab Simulink interface. Fig. 13 presents the response of the system with PID controller and without controller when the system input is square wave signal from pulse generator. It can be observed that the controller controls the PZT to give the desired output (blue line) which track the reference (green line) while the one without controller did not give the desired output (red line) of Fig. 13. Figure 14 shows the response of the PZT

dynamic model when the step input was applied with and without PID controller.

3.0 RESULTS AND DISCUSSION

The result displayed in Figure 12 shows a comparison between non-dynamic PZT control with PID controller and the one without controller with step input. It can be seen that the PID controller controls the system to follow the reference input. Figure 13 displays the comparison between the dynamic PZT control with PID controller and the one without controller using square wave from pulse generator as input. Figure 14 also compares between the dynamic PZT with PID controller and the one without controller when the step input was applied.

4.0 CONCLUSION

The dynamic and non-dynamic models of piezoelectric actuator was efficiently developed with experimental data (system identification) and control using PID controller in Matlab Simulink. The non-dynamic equation developed will be suitably used to micro displacement such as micro positioning. The dynamic model developed is suitable to be used in dynamic applications such as micro actuation, and micro fluidic (micro pump). Simulation using Matlab Simulink was used to validate the experiment. The hysteresis was reduced by 90 % and the vibration was reduced to 97 %.

Acknowledgement

The research was supported by the Ministry of Higher Education of Malaysia (grant Nos. 4L640 and 4F351), and Universiti Teknologi Malaysia (grant Nos. 03G47, 02G46, 03H82, and 03H80); we thank them for funding this project and for their endless support. Special appreciation to my family (Mahe Bala, Nasir Bala and Jadidu Bala), and members of Micro-Nano Mechatronics research group (Universiti of Teknologi Malaysia) for their continuous support.

References

- [1] J. Torres and H. H. Asada. 2014. High-Gain, High Transmissibility PZT Displacement Amplification Using a Rolling-Contact Buckling Mechanism and Preload Compensation Springs. *IEEE Trans. Robot.* Aug 2014. 30(4): 781–791.
- [2] Matsubara, M. Maeda and I. Yamaji. 2014. Vibration Suppression of Boring Bar by Piezoelectric Actuators and LR Circuit. *CIRP Ann. - Manuf. Technol.* 63(1): 373–376.
- [3] Abis, F. Unal and A. Muga. 2011. Active Vibration Control with Piezoelectric Actuator on a Lathe Machine with a Gain Controller. *IEEE International Conference on Mechatronics.* 19–22.
- [4] C.-Y. S. and M. O. Jian Wang. 2003. Theoretic Modeling and

- Adaptive Control for Two Degree-Of-Freedom Piezo-Electric Actuated Chatter Suppression System. 42nd IEEE Conference on Decision and Control. 4315-4320.
- [5] T. Zhang, H. G. Li and G. P. Cai. 2013. Hysteresis Identification and Adaptive Vibration Control for a Smart Cantilever Beam by a Piezoelectric Actuator. Elsevier. Dec 2013. 203: 168-175.
- [6] F. M. and A. S. M. khaled Joujou. 2008. Experimental Fuzzy Logic Active Vibration Control. 5th International Symposium on Mechatronics and its Applications (ISMA08). 6-12.
- [7] W. Li and X. Chen. 2013. Compensation of Hysteresis in Piezoelectric Actuators without Dynamics Modeling. *Sensors Actuators A Phys.* 199: 89-97.
- [8] F. Heidary and M. Reza Eslami. 2006. Piezo-Control of Forced Vibrations of a Thermoelastic Composite Plate. *Compos. Struct.* 74(1): 99-105.
- [9] M. N. M, Z. Mohamed, A. M. Abdullahi, M. R. Ahmad and A. R. Husain. 2014. Dynamic Hysteresis Based Modeling of Piezoelectric Actuators. *J. Teknol.* 67(5): 9-13.
- [10] B. B. Muhammad. 2015. Modelling and Vibration Control of Piezoelectric Actuator. Universiti Teknologi Malaysia.
- [11] S. T. A. Ctuators, B. Hu, M. Z. Rahim and S. Ding. 2015. Gap Control Of Electrical Discharge Grinding With High Bandwidth Dual Stage Actuators. *J. Teknol.* 75(11): 101-106.
- [12] R. Dong, Y. Tan and Y. Xie. 2016. Identification of Micropositioning Stage with Piezoelectric Actuators. *Mech. Syst. Signal Process.* 75: 618-630.
- A. Michael and C. Y. Kwok. 2014. Piezoelectric Micro-Lens Actuator. *Sensors Actuators A Phys.* 236: 116-129.
- [13] R. Svecko and D. Kusic. 2015. Feedforward Neural Network Position Control of a Piezoelectric Actuator Based on A BAT Search Algorithm. *Expert Syst. Appl.* 42(13): 5416-5423.
- [14] Y. Peng, S. Ito, Y. Shimizu, T. Azuma, W. Gao and E. Niwa. 2014. A Cr-N Thin Film Displacement Sensor for Precision Positioning of a Micro-Stage. *Sensors Actuators, A Phys.* 211.
- [15] J. Chen, C. Zhang, M. Xu, Y. Zi and X. Zhang. 2015. Rhombic Micro-Displacement Amplifier for Piezoelectric Actuator and Its Linear and Hybrid Model. *Mech. Syst. Signal Process.* 50-51: 580-593.
- [16] H. GhafariRad, S. M. Rezaei, M. Zareinejad and A. Abdullah. 2011. Adaptive Robust Control for Micropositioning of Piezoelectric Actuators with Environment Force Estimation. *Trans. Inst. Meas. Control.* 34(8): 956-965.
- [17] J. Kim and S. Nam. 1995. Development of a Micro-Positioning Grinding Table Using Piezoelectric Voltage Feedback. *J. Eng. Manuf.* 209(6): 469-474.
- [18] V.-T. Liu, H.-C. Huang, C.-L. Lin and Z.-J. Jian. 2007. Neural Net-based Modeling and Control of a Micro-positioning Platform Using Piezoelectric Actuators. *J. Vib. Control.* 13(3): 309-325.
- [19] Y.-T. Liu and C.-K. Wang. 2009. A Study of the Characteristics of a One-Degree-Of-Freedom Positioning Device Using Spring-Mounted Piezoelectric Actuators. *Proc. Inst. Mech. Eng. Part C J. Mech. Eng. Sci.* 223(9): 2017-2027.
- [20] W. Zhu, Z. Wang, X. Sun, and Z. Zhang. 2001. A Multilayer Inplane Bending Piezoelectric Actuator for Dual-Stage Head-Positioning Control. *J. Mater. Sci. Mater. Electron.* 12(2): 111-116.
- [21] Z. He, G. Guo, L. Feng, W. E. Wong and H. T. Loh. 2006. Microactuation Mechanism with Piezoelectric Element for Magnetic Recording Head Positioning For Spin Stand. *Proc. Inst. Mech. Eng. Part C J. Mech. Eng. Sci.* 220(9): 1455-1461.
- [22] P. Smithmaitrie and H. S. Tzou. 2005. Electro-dynamics, Micro-Actuation and Design of Arc Stators in an Ultrasonic Curvilinear Motor. *J. Sound Vib.* 284(3-5): 635-650.
- [23] W. K. Chai, Y. Han, K. Higuchi and H. S. Tzou. 2006. Micro-Actuation Characteristics of Rocket Conical Shell Sections. *J. Sound Vib.* 293(1-2): 286-298.
- [24] C.-H. Cheng, A.-S. Yang, C.-J. Lin and W.-J. Huang. 2015. Characteristic Studies of a Novel Piezoelectric Impedance Micropump. *Microsyst. Technol.* 1-9.
- [25] J. Shemesh, A. Bransky and M. Khoury. 2010. Advanced Microfluidic Droplet Manipulation Based On Piezoelectric Actuation. *Biomed Microdevices.* 12(5): 907-914.
- [26] Y. Le and N Hsu. 2009. Equivalent Electrical Network for Performance Characterization of Piezoelectric Peristaltic Micropump. *Microfluid Nanofluidics.* 7(2): 237-248.
- [27] M. Y. Ali, C. Kuang, J. Khan and G. Wang. 2010. A Dynamic Piezoelectric Micropumping Phenomenon. *Microfluid Nanofluidics.* 9(2-3): 385-396.
- [28] P. H. Cazorla, O. Fuchs, M. Cochet, S. Maubert, G. Le Rhun, P. Robert, Y. Fouillet and E. Defay. 2014. Piezoelectric Micro-Pump with PZT Thin Film for Low Consumption Microfluidic Devices. *Procedia Eng.* 87: 488-491.
- [29] D. S. Lee, J. S. Ko and Y. T. Kim. 2004. Bidirectional Pumping Properties of a Peristaltic Piezoelectric Micropump with Simple Design and Chemical Resistance. *Thin Solid Films.* 468(1-2): 285-290.
- [30] J. Kan, K. Tang, G. Liu, G. Zhu and C. Shao. 2008. Development of Serial-Connection Piezoelectric Pumps. *Sensors Actuators. A Phys.* 144(2): 321-327.